

- strongest pressure dependence parallels the strongest density changes (and hence the strongest changes in molecular interactions). Because fluid pressure rather than density is the commonly used variable in geochemistry, the relation to pressure has been kept throughout the present communication.
13. L. Haar, J. S. Gallagher, G. S. Kell, *NBS/NRC Steam Tables* (1983).
 14. R. N. Clayton *et al.*, *Geochim. Cosmochim. Acta* **39**, 1197 (1975).
 15. C. M. Graham, S. M. F. Sheppard, T. H. Heaton, *ibid.* **44**, 353 (1980).
 16. T. W. Vennemann and J. R. O'Neil, *ibid.* **60**, 2437 (1996).
 17. H. E. Suess, *Z. Naturforsch.* **4a**, 328 (1949); E. Cerrai *et al.*, *Chem. Eng. Prog. Symp. Ser.* **50**, 271 (1958).
 18. P. Richet, Y. Bottinga, M. Javoy, *Annu. Rev. Earth Planet. Sci.* **5**, 65 (1977).
 19. J. Horita and D. J. Wesolowski, *Geochim. Cosmochim. Acta* **58**, 3425 (1994).
 20. Evidence for such clusters comes from the low-pressure Raman spectra of Frantz *et al.* (5), as well as from molecular dynamics simulations [Y. Guissani and B. Guillot, *J. Chem. Phys.* **98**, 8221 (1993)].
 21. The molecular dynamics simulations were carried out with the SPC/E water model that has been shown to accurately reproduce the liquid-vapor curve and the critical parameters as well as many other properties of real water [Y. Guissani and B. Guillot, *J. Chem. Phys.* **98**, 8221 (1993); J. Alejandre, D. J. Tildesley, G. A. Chapela, *ibid.* **102**, 4574 (1994)]. Simulations were done with 1000 SPC/E water molecules in a cubic box with periodic boundary conditions in the NVT ensemble. Densities were chosen according to the two studies mentioned above. Long-range forces were treated with Ewald summation. Systems were allowed to equilibrate for at least 25 ps, and simulation runs were at least 50 ps. When calculating the fractions of the various clusters from the positions of the molecules in the simulation box, geometrical criteria for the identification of the clusters were applied. It was assumed that a molecule belongs to a cluster when its oxygen is located within a distance smaller than the position of the first minimum of the oxygen-oxygen radial distribution function (typically 4.0 to 4.2 Å). The calculations of the vibrational spectra of the clusters were done with density functional methods as implemented in Gaussian94 (M. J. Frisch *et al.*, Gaussian94, Gaussian Inc., Pittsburgh, PA, 1995). The BLYP functional in combination with the 6-31G** basis set was used. This method yields precise frequencies that are numerically very close to the spectroscopic values [see, for example, A. P. Scott and L. Radom, *J. Phys. Chem.* **100**, 16502 (1996)]. For each cluster, after the geometry optimization, one calculation was carried out with ¹⁶O and H only. Then, a series of calculations were carried out in each of which one of the various hydrogens was substituted by D. The fractionation relative to the monomer was calculated for all these various possibilities, and the arithmetic mean of the 1000 ln $\alpha_{\text{cluster-monomer}}$ was taken as the average cluster-monomer fractionation. Calculations at the MP2/6-31G** level gave essentially identical fractionation factors when the scaling factors given by Scott and Radom were used. The vapor-monomer fractionation is directly calculated from these results. Changing parameters like the geometric definition of clusters within reasonable limits indicate uncertainties in this approach of less than 5 per mil at 400°C and of about 1 per mil at 200°C.
 22. Furthermore, pressure effects explain many details in the data set of Graham *et al.* (15) that otherwise are not understandable. At 250°C their 400-MPa fractionation curve lies ~4 to 5 per mil higher than the 200-MPa curve. A rough extrapolation of Fig. 1A to higher pressures predicts a similar, though slightly smaller, shift. At 350°C, the same equilibrium fractionation was measured for the two different pressures. Inspection of Fig. 1B reveals a straightforward explanation: At 200 MPa and 350°C, the contour lines of the pressure effect lie very close together, and a temperature variation of 5°C [the stated uncertainty of Graham *et al.* (15)] can cause a change in the fractionation by a few per mil.
 23. T. Suzuoki and S. Epstein, *Geochim. Cosmochim. Acta* **40**, 1229 (1976). These authors did not give information about the pressure in their experiments, but in the light of the present results, their 400° and 450°C data are likely to have been generated at about 250 to 400 bars.
 24. C. M. Graham, R. S. Harmon, S. M. F. Sheppard, *Am. Mineral.* **69**, 128 (1984).
 25. H. A. Gilg and S. M. F. Sheppard, *Geochim. Cosmochim. Acta* **60**, 3, 529 (1996).
 26. R. E. Stoffregen, R. O. Rye, M. D. Wasserman, *ibid.* **58**, 903 (1994).
 27. T. Driesner, thesis, Eidgenössische Technische Hochschule-Zürich (1996); K. Shmulovich *et al.*, *Terra Nova* **9**, 540 (1997).

10 April 1997; accepted 19 June 1997

Paleostress in Cratonic North America: Implications for Deformation of Continental Interiors

Ben A. van der Pluijm, John P. Craddock, Brita R. Graham,
John H. Harris

Compressive paleostresses, as recorded by twinned calcite in carbonate rocks that cover cratonic northwestern North America, are perpendicular to the orogenic front of the Late Cretaceous to Early Cenozoic Sevier fold-thrust belt. Inferred differential stresses decrease from ~100 megapascals (MPa) at the orogenic front to ~20 MPa up to 2000 kilometers inland. New analyses near the Late Paleozoic Appalachian front refine earlier results from the eastern Midcontinent. The Appalachian and Sevier stress data in North America's continental interior are remarkably similar in spite of distinctly different tectonic properties. This suggests that continental interior stresses are largely insensitive to tectonic characteristics of compressive plate margins and that far-field stress transmission is filtered by deformation styles in mountain belts.

A basic tenet of plate tectonics is that deformation is concentrated at plate margins, whereas plate interiors are rigid and undeformable (1). This basic assumption is supported by many geologic observations, such as the location of major earthquake activity, certain types of volcanism, and present-day mountain-building processes. However, continental interiors are increasingly recognized as sensitive recorders of plate tectonic activity (2, 3). For example, Late Paleozoic plate interactions at the Appalachian margin of North America produced fault reactivation, folds and detachments, and joint and cleavage fabrics in the eastern Midcontinent region of the United States (4, 5). We present data from the western part of the continent, which is characterized by Mesozoic-Cenozoic convergence between the Farallon and North American plates that resulted in the formation of the Sevier fold-thrust belt (Sevier f., Fig. 1). In addition, we obtained results from a 300-km section in the eastern Midcontinent to better constrain the nature of paleostress decrease near orogenic fronts (Appalachian f., Fig. 1).

Our regional strain and paleostress his-

tory uses the twinning of calcite in limestone, cement, and veins of the Sevier fold-thrust belt and its foreland, younger basement-cored (Laramide) structures and old adjacent tectonic provinces. Calcite grains can twin mechanically at low differential stress (<20 MPa) in a crystal-plastic process that is largely independent of temperature and normal stress magnitude at shallow crustal conditions. Twinning occurs along one of three glide planes, and calcite strain-hardens once twins have formed; further twinning is possible along either of the remaining two planes at higher stresses, provided that stress is oriented >45° from the initial stress orientation (6).

The orientation (7) and magnitude of paleostresses responsible for twinning can be calculated (8); magnitude errors are within 20%. Strain determinations using the Groshong method (9) are quite accurate for finite strains less than ~15%. This method also computes negative and positive expected values (NEVs and PEVs, respectively) for all the twinned grains in a sample. A NEV indicates that a grain was unfavorably oriented relative to the stress that caused most of the other grains in a sample to twin. High NEV percentages (>35%) may indicate that a second, non-coaxial strain event occurred, and these two events can be analyzed separately. We only used samples that are characterized by low

B. A. van der Pluijm, B. R. Graham, J. H. Harris, Department of Geological Sciences, University of Michigan, Ann Arbor, MI 48109, USA.

J. P. Craddock, Geology Department, Macalester College, St. Paul, MN 55105, USA.

NEVs. Limestones within the Idaho-Wyoming fold-thrust belt preserve a fabric that was produced during thrust displacement (10). In contrast, calcite veins across the belt record high differential stresses and shortening strains, with variable orientations of fabrics that reflect local complexities. We therefore excluded vein data from our analysis as well.

We analyzed 42 sites in Paleozoic limestones and veins from the Beartooth, Wind River, Owl Creek, Bighorn, and Black Hills ranges and the Heart Mountain area, complementing data from the Bighorn Mountains (11), Teton-Gros Ventre Range (12), Wind River Range, and Wind River basin (13) (Fig. 2A). Calcite twins from limestones in Laramide uplifts preserve a regional fabric that implies shortening in an approximately ENE-WSW direction, even though in some cases Laramide deformation involved uplift and thrust transport from north to south (for example, Owl Creek Range) (14). Samples from folds flanking the Wind River Range record an E-W fabric. Twins in calcite veins have subhorizontal N-S fabrics regardless of the vein orientation.

Samples from the Cretaceous Greenhorn Limestone in western Minnesota, near Brown's Valley at the southeast end of Traverse Lake, represent the easternmost exposures of carbonate rocks of the Cretaceous Seaway. This unit is a flat-lying, locally sparry limestone that preserves a horizontal E-W fabric. Minnesota also contains Paleozoic limestone that, in places, underlies Cretaceous sedimentary rocks. Here, however, calcite twins are oriented roughly perpendicular to the E-W Sevier fabric and preserve an orientation associated with deformation in the Appalachian-Ouachita orogen that is ~1500 km away (4).

Mesozoic to Early Cenozoic deformation

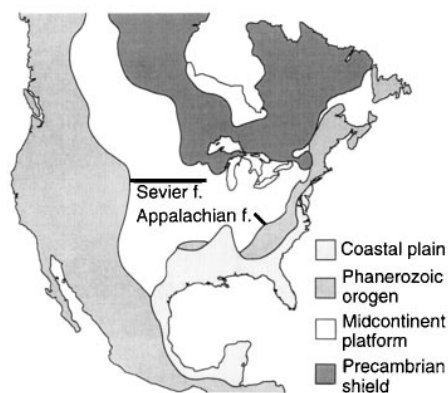


Fig. 1. Generalized tectonic map of North America showing Phanerozoic orogens and the continental interior. Calcite twinning data were obtained along the two sections shown; the Appalachian section complements previously published data (4) that are included in Fig. 2C.

in the western margin of North America formed the Idaho-Wyoming (Sevier) fold-thrust belt (15), the proximal Green River foreland basin (16) and distal foreland basins, and Laramide basement uplifts (17). The older part of the Sevier belt formed near the plate margin, with thrust translation and age progression toward the east. Farther inland, basement blocks were uplifted in the Laramide orogeny and crustal shortening was generally oriented NE-SW.

The data from western North America show that shortening strains decrease from ~6% at the Sevier orogenic front to <2% in the cratonic interior, but the values are scattered. Differential stress data (Fig. 2A) steadily decrease from ~100 MPa at the orogenic front to ~20 MPa in western Minnesota. These data show that a regional shortening fabric extended away from the western plate boundary as far as Minnesota, indicating that orogenic stresses were transmitted over more than 2000 km. Within ~300 km of the exposed orogenic front, differential stress values decrease to ~30 MPa. Over the entire traverse, the results fit the logarithmic relation $\sigma_d = -11 \ln D + 105$, where D is distance in kilometers ($R = 0.83$; 21 sites).

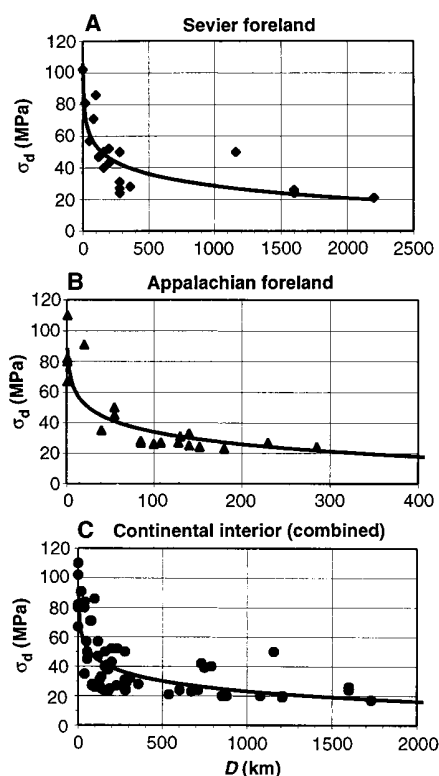


Fig. 2. Differential stress magnitudes inferred from twinned calcite in limestones in the foreland of the Sevier orogen (A) and in the foreland of the Appalachian orogen (B) and from combined results from this study and previously published Appalachian-Ouachita data (C).

To examine whether the rapid paleostress drop in the Sevier data and a similar pattern in samples from the eastern Midcontinent are a general feature of continental deformation, we studied a suite of samples from Tennessee to Indiana (Fig. 1). Inferred differential stresses from a single traverse (Fig. 2B) change from ~110 MPa at the orogenic front to ~30 MPa at 200 km inland. These data can be fitted by $\sigma_d = -12 \ln D + 87$ ($R = 0.88$; 22 sites); corresponding strain values decrease from >8% to ~2% over this distance. These results complement previous data from the Appalachian-Ouachita foreland (3) that collectively fit the relation $\sigma_d = -10 \ln D + 89$ ($R = 0.82$; 49 sites).

Our data imply that orogenic stresses at plate margins are transmitted over distances up to 2000 km into the continental interior (18). Moreover, the Sevier and Appalachian-Ouachita data sets are remarkably similar; combined (Fig. 2C), they fit the relation $\sigma_d = -10 \ln D + 92$ ($R = 0.81$; 70 sites). Based on the contrasting characteristics between the Late Paleozoic Appalachian-Ouachita belt and Late Mesozoic Sevier belt, we conclude that the stress state of the continental interior seems independent of the setting, style, and age of plate margin tectonics, as well as of orogenic architecture. This indicates that tectonic properties such as obliquity of convergence, slab dip, and lateral extent of colliding elements may not be reflected in plate interior stresses. Rather, mountain belts act as "filters" for stress transmission, while their internal architecture may reflect variations in stress state at the plate margin. Thus, the stress state of continental interiors is independent of the detailed nature of plate activity at compressional margins, and plate tectonic stresses are transmitted across most of the continental interior with values that primarily depend on the distance from the exposed orogenic front. Transmitted differential stresses in continental interiors on the order of tens of megapascals also imply that intraplate fault reactivation (and earthquake triggering) are mainly dependent on the orientation of (weak) fault zones (19) relative to the plate margin, and that deformation of continental interiors can be represented by relatively simple rheologic models (20).

REFERENCES AND NOTES

1. D. McKenzie and R. L. Parker, *Nature* **216**, 1276 (1967).
2. M. L. Zoback *et al.*, *ibid.* **341**, 291 (1989).
3. S. Marshak and B. A. van der Pluijm, in *Earth Structure*, B. A. van der Pluijm and S. Marshak, Eds. (WCB/McGraw-Hill, Dubuque, IA, 1997), pp. 465-472.
4. J. P. Craddock, M. Jackson, B. A. van der Pluijm, R. Versical, *Tectonics* **12**, 257 (1993).

5. S. Marshak and T. Paulson, *Geology* **24**, 151 (1996).
6. M. Burkhard, *J. Struct. Geol.* **15**, 351 (1993).
7. F. J. Turner, *Am. J. Sci.* **251**, 276 (1953).
8. W. R. Jamison and J. H. Spang, *Bull. Geol. Soc. Am.* **87**, 868 (1976).
9. R. H. Groshong Jr., L. W. Teufel, C. M. Gasteiger, *ibid.* **95**, 357 (1984).
10. J. P. Craddock, *Geol. Soc. Am. Mem.* **179**, 125 (1992).
11. P. H. Hennings and J. H. Spang, *Geol. Soc. Am. Abstr. Prog.* **18**, 635 (1986).
12. J. P. Craddock, A. Kopania, D. V. Wiltschko, *Geol. Soc. Am. Mem.* **171**, 333 (1988).
13. J. J. Willis and R. H. Groshong Jr., *Wyom. Geol. Assoc. Guidebook*, 95 (1993).
14. R. J. Varga, *Geology* **21**, 1115 (1993).
15. D. V. Wiltschko and J. A. Dorr, *Bull. Am. Assoc. Pet. Geol.* **67**, 1304 (1983).
16. J. A. Dorr Jr., D. R. Sparing, J. R. Steidtmann, *Geol. Soc. Am. Spec. Pap.* **177**, 82 (1977).
17. T. E. Jordan, *Bull. Am. Assoc. Pet. Geol.* **65**, 2506 (1981).
18. The absence of any overprint in calcite by the contemporaneous stress field and Mesozoic extension in the west indicates that calcite strain-hardens once it twins. Moreover, carbonates in other tectonic provinces of North America show distinctly different patterns, unrelated to either Appalachian-Ouachita or Sevier stresses (4).
19. N. H. Sleep and M. L. Blanpied, *Nature* **359**, 687 (1992).
20. P. England, G. Houseman, L. Sonder, *J. Geophys. Res.* **90**, 3551 (1985).
21. We thank the Pew Charitable Trust, the Blandin Foundation, the Huron Mountain Wildlife Foundation, and NSF for grants EAR 90-04181 and ACS-PRF 27461-AC8. Comments by R. Van der Voo and three anonymous reviewers are greatly appreciated.

31 March 1997; accepted 2 June 1997

Variability in Radiocarbon Ages of Individual Organic Compounds from Marine Sediments

Timothy I. Eglinton,* Bryan C. Benitez-Nelson, Ann Pearson, Ann P. McNichol, James E. Bauer, Ellen R. M. Druffel

Organic carbon (OC) from multiple sources can be delivered contemporaneously to aquatic sediments. The influence of different OC inputs on carbon-14-based sediment chronologies is illustrated in the carbon-14 ages of purified, source-specific (biomarker) organic compounds from near-surface sediments underlying two contrasting marine systems, the Black Sea and the Arabian Sea. In the Black Sea, isotopic heterogeneity of *n*-alkanes indicated that OC was contributed from both fossil and contemporary sources. Compounds reflecting different source inputs to the Arabian Sea exhibit a 10,000-year range in conventional carbon-14 ages. Radiocarbon measurements of biomarkers of marine photoautotrophy enable sediment chronologies to be constructed independent of detrital OC influences.

Molecular-level studies of organic compounds in marine sediments can provide a wealth of information on the carbon cycle in past and present-day oceans as well as information on the depositional setting and origin of organic matter. Of greatest utility are lipid biomarkers that are specific to individual or a restricted range of organisms and that are sufficiently refractory to be preserved in sediments. Three characteristic features of individual organic compounds are currently exploited by biogeochemists: precise molecular structure, absolute or relative abundance, and stable carbon isotopic composition. A fourth feature, the radiocarbon content, has been added to the list (1). The ¹⁴C content provides a means to evaluate the source and fate of natural and anthropogenic organic compounds in the biogeosphere.

Organic materials from various sources

and with different ages are deposited concurrently in marine sediments. This is particularly the case near continents where fresh vascular plant debris, soil organic matter, and OC eroded from sedimentary rocks may be deposited together with autochthonous biomass synthesized in the water column. The construction of carbon budgets and sediment chronologies based on ¹⁴C measurements of total organic carbon (TOC) depends on being able to accurately quantify these inputs. The ages of specific OC inputs and their influence on TOC ¹⁴C ages have remained elusive. Measurements of different compound classes in sediments have indicated that ¹⁴C contents are heterogeneous (2), but it is only at the biomarker level that these variations are fully expressed and can be attributed to specific inputs.

Here we present an assessment of radiocarbon ages measured in individual biomarkers from two contrasting marine sedimentary systems. The Black Sea is a stratified anoxic marine basin, and the Arabian Sea is a highly productive system supported by intense seasonal upwelling. Organic carbon-rich sediments accumulating in both seas are strongly influenced by terrigenous inputs. Numerous large rivers drain into the western Black Sea and affect the hydrography and geochemistry of this system (3), whereas eolian dust

associated with seasonal monsoons is the primary mode of supply of continental OC to the Arabian Sea (4).

In the Black Sea, we studied laminated OC-rich (TOC, 5.5%) sediments at a depth of 4 to 7 cm recovered by a Mk-III box corer (BC4, station 2; 42°51'N, 31°57'E, at a water depth of 2129 m) during leg 134-9 of the 1988 R/V *Knorr* expedition. In the Arabian Sea, we studied a sediment sample (box core 6BC, depth of 2 to 4 cm; TOC, 6.7%) obtained from the Oman upwelling region in the Arabian Sea (17°48.7'N, 57°30.3'E, at a water depth of 747 m) during leg TN041 of the R/V *T.G. Thompson* expedition in 1994. We measured the natural ¹⁴C content of specific biomarker compounds chosen to reflect both autochthonous and allochthonous inputs (5) in order to evaluate the magnitude and source of age variation in these components of sedimentary organic matter.

We selected a series of long chain (C₃₇₋₃₉) alkenes (compounds i in Table 1), the dominant unsaturated hydrocarbons in the Black Sea lipid extract, for radiocarbon dating as biomarkers of marine photoautotrophy. These compounds are derived from prymnesiophyte algae, such as the coccolithophorid *Emiliania huxleyi*, a major phytoplankton and important contributor to sinking particulate matter in the contemporary Black Sea (6). An autochthonous origin for these compounds is supported by their δ¹³C values (Table 1), which are consistent with values for lipids from marine phytoplankton (7). The similarity in both ¹³C values and the conventional ¹⁴C ages (8) (Table 1) between the alkenes [average δ¹³C = -25.5 per mil; 950 years before the present (B.P.), respectively] and TOC (δ¹³C = -24.2 per mil; 880 years B.P.) suggests that modern photoautotrophic biomass is a major component of the bulk OC in these sediments. The similarity in ¹⁴C ages between prymnesiophyte alkenes and TOC also suggests that, contrary to previous assumptions (9), older detrital OC inputs have a minimal influence on the ¹⁴C_{TOC} age of late Holocene Black Sea sediments. Conversion of conventional radiocarbon ages to reservoir-corrected ages for marine carbon re-

T. I. Eglinton, B. C. Benitez-Nelson, A. Pearson, Department of Marine Chemistry and Geochemistry, Woods Hole Oceanographic Institution, Woods Hole, MA 02543, USA.

A. P. McNichol, National Ocean Sciences Accelerator Mass Spectrometry Facility, Woods Hole Oceanographic Institution, Woods Hole, MA 02543, USA.

J. E. Bauer, School of Marine Science, College of William and Mary, Gloucester Point, VA 23062, USA.

E. R. M. Druffel, Department of Earth System Science, University of California, Irvine, CA 92697, USA.

*To whom correspondence should be addressed.